THE JOURNAL OF BIOLOGICAL CHEMISTRY VOL. 283, NO. 38, pp. 25971–25978, September 19, 2008

Evidence That Two Enzyme-derived Histidine Ligands Are Sufficient for Iron Binding and Catalysis by Factor Inhibiting HIF (FIH)*[S]

Received for publication, July 1, 2008 Published, JBC Papers in Press, July 8, 2008, DOI 10.1074/jbc.M804999200

Kirsty S. Hewitson[1,2], Samantha L. Holmes[1], Dominic Ehrismann[1,3], Adam P. Hardy, Rasheduzzaman Chowdhury, Christopher J. Schofield[4], and Michael A. McDonough[5]

From the Chemistry Research Laboratory, The Department of Chemistry, University of Oxford, Mansfield Road, Oxford OX1 3TA, United Kingdom

A 2-His-1-carboxylate triad of iron binding residues is present in many non-heme iron oxygenases including the Fe(II) and 2-oxoglutarate (2OG)-dependent dioxygenases. Three variants (D201A, D201E, and D201G) of the iron binding Asp-201 residue of an asparaginyl hydroxylase, factor inhibiting HIF (FIH), were made and analyzed. FIH-D201A and FIH-D201E did not catalyze asparaginyl hydroxylation, but in the presence of a reducing agent, they displayed enhanced 2OG turnover when compared with wild-type FIH. Turnover of 2OG by FIH-D201A was significantly stimulated by the addition of HIF-1$\alpha_{786-826}$ peptide. Like FIH-D201A and D201E, the D201G variant enhanced 2OG turnover but rather unexpectedly catalyzed asparaginyl hydroxylation. Crystal structures of the FIH-D201A and D201G variants in complex with Fe(II)/Zn(II), 2OG, and HIF-1$\alpha_{786-826/788-806}$ implied that only two FIH-based residues (His-199 and His-279) are required for metal binding. The results indicate that variation of 2OG-dependent dioxygenase iron-ligating residues as a means of functional assignment should be treated with caution. The results are of mechanistic interest in the light of recent biochemical and structural analyses of non-heme iron and 2OG-dependent halogenases that are similar to the FIH-D201A/G variants in that they use only two His-residues to ligate iron.

The 2-His-1-carboxylate iron binding triad (H*X*(D/E) . . . H) is an extensively conserved feature of the active site of the non-heme iron-dependent oxygenases and oxidases, including the 2OG[6]-dependent dioxygenase family (2OG oxygenases). Crystallographic and spectroscopic studies imply that the enzyme·Fe·2OG intermediate has an octahedral metal coordination, with three of the coordination sites occupied by the 2-oxo-acid of 2OG and a water molecule. In some cases, binding of substrate to this complex has been shown to induce loss of the iron bound water so enabling dioxygen binding. Oxidative decarboxylation of 2OG results in the formation of a ferryl species (Fe(VI)=O) that effects oxidation of the substrate/co-substrate with the regeneration of Fe(II) at the active site (for review, see Refs. 1–3). In addition, spectroscopic studies have demonstrated that interaction of the non-iron-ligated oxygen atom of the carboxylate side chain of the metal binding Asp/Glu residue with the iron bound water molecule has a role in oxygen activation (4).

Hydroxylation is the most common reaction catalyzed by the 2OG oxygenases, but family members also catalyze other oxidative reactions including demethylations, desaturations, epoxidations, and rearrangements. Related enzymes, which do not employ 2OG as a co-substrate, have been shown to catalyze oxidative fragmentations and cyclization reactions (for review, see Refs. 2 and 5). Recently, two 2OG oxygenases have been reported to catalyze oxidative halogenations (6, 7); the structure of one of these halogenases, SyrB2, revealed that the iron was coordinated by only two enzyme-derived His residues (8). The carboxylate-bearing residue found in all prior 2OG oxygenase structures was substituted by an Ala in SyrB2 apparently leaving sufficient space for a chloride ion to fill the vacant iron coordination site.

Four 2OG oxygenases are known to be involved in regulation of the hypoxic response in humans via the post-translational hydroxylation of specific residues in the α-subunit of hypoxia-inducible factor (HIF): three prolyl hydroxylases (9, 10) and an asparagine hydroxylase (FIH, factor inhibiting HIF (11–13)). Hydroxylation of specific proline residues signals for the proteolytic destruction of HIF-α (9, 10), whereas hydroxylation of an asparagine residue (Asn-803 in human HIF-1α) (Fig. 1) in the C-terminal transactivation domain blocks recruitment of

* This work was supported by grants from the Wellcome Trust, the Engineering and Physical Sciences Research Council, and the Biotechnology and Biological Sciences Research Council for funding. The costs of publication of this article were defrayed in part by the payment of page charges. This article must therefore be hereby marked "*advertisement*" in accordance with 18 U.S.C. Section 1734 solely to indicate this fact.

The atomic coordinates and structure factors (codes 2ILM, 3D8C) have been deposited in the Protein Data Bank, Research Collaboratory for Structural Bioinformatics, Rutgers University, New Brunswick, NJ (http://www.rcsb.org/).

[S] The on-line version of this article (available at http://www.jbc.org) contains a supplemental table and four supplemental figures.

[1] These authors contributed equally to this work.

[2] Supported by a Glasstone Fellowship during the course of this work.

[3] A recipient of a Fellowship from the Roche Research Foundation and the Freiwillige Akademische Gesellschaft.

[4] To whom correspondence may be addressed. Tel.: 44-1865-275625; Fax: 44-1865-285002; E-mail: christopher.schofield@chem.ox.ac.uk.

[5] To whom correspondence may be addressed. Tel.: 44-1865-275629; Fax: 44-1865-285002; E-mail: michael.mcdonough@chem.ox.ac.uk.

[6] The abbreviations used are: 2OG, 2-oxoglutarate; DTT, dithiothreitol; FIH, factor inhibiting HIF; HIF, hypoxia-inducible transcription factor; PDB, Protein Data Bank; GST, glutathione *S*-transferase; MS, mass spectrometry; MALDI, matrix-assisted laser desorption/ionization; CREB, cAMP-response element-binding protein; WT, wild type.

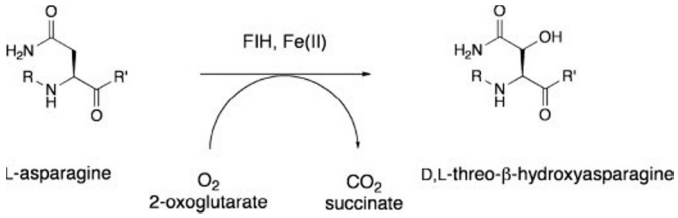

FIGURE 1. **The reaction catalyzed by wild-type FIH (and FIH-D201G). hydroxylation of the β-carbon of Asn-803 within the C-terminal transactivation domain of HIF-1α.** The reaction requires Fe(II) as a cofactor and dioxygen and 2OG as co-substrates that are converted to succinate and carbon dioxide concomitant with hydroxylation of HIF-1α substrate. For the FIH-D201A/E variants, 2OG decarboxylation is uncoupled from the hydroxylation of HIF-1α substrate and is stimulated by the presence of a reducing agent (ascorbate or DTT).

the p300/CREB-binding protein co-activators (11–13) (for review, see Refs. 14 and 15).

Studies on the iron cofactor binding residues of FIH have supported the assignment of FIH as a 2OG oxygenase and enabled identification of the iron binding residues as His-199, Asp-201, and His-279. Lando *et al.* (12) demonstrated that substitution of either His-199 or Asp-201 to alanine residues ablated FIH activity in cells. Crystallographic analyses confirmed the assignment of the iron binding residues (16–18). A structure of dimeric FIH in complex with Fe(II), 2OG, and HIF-1$\alpha_{786-826}$ revealed that the side-chain carboxylate of FIH Asp-201 not only coordinates the iron via one oxygen, but that its other oxygen is positioned to accept a hydrogen bond from an Fe(II)-bound water molecule; upon substrate binding, the interaction of the water is apparently weakened because Asp-201 is repositioned to form a hydrogen bond with the backbone amide nitrogen of HIF-1α Asn-803 as observed in the crystal structures (Fig. 2) (17).

We report here that although FIH-D201A and FIH-D201E do not catalyze HIF-1α hydroxylation, under appropriate conditions, these enzymes do catalyze enhanced 2OG turnover when compared with the wild-type FIH. Surprisingly, the FIH-D201G mutant catalyzes asparaginyl hydroxylation at comparable levels to wild-type FIH. Crystal structures of FIH-D201A·Fe(II)·2OG·HIF-1$\alpha_{786-826}$ and D201G·Zn(II)·2OG·HIF-1$\alpha_{788-806}$ reveal that the only FIH-based ligands required to bind iron are His-199 and His-279. Together with the recent studies on 2OG halogenases (6, 7) and spectroscopic analyses (4), our results indicate that there is more flexibility in the iron coordination chemistry of 2OG oxygenases than previously thought.

EXPERIMENTAL PROCEDURES

FIH Mutations—The FIH-D201A/E/G, W296R, and L340R variants were produced from the wild-type construct using the QuikChange site-directed mutagenesis kit (Stratagene). The primers used were: D201A, forward, 5′-GCT CAC TAT **GCT** GAG CAG CAG AAC-3′; reverse, 5′-CTG CTG CTC **AGC** ATA GTG AGC AGG-3′; D201E, forward, 5′-GCT CAC TAT **GAG** GAG CAG CAG AAC-3′; reverse, 5′-CTG CTG CTC **CTC** ATA GTG AGC AGG-3′; D201G, forward, 5′-GTG ACA CCT GCT CAC TAT **GGC** GAG CAG CAG AAC-3′; reverse, 5′-GTT CTG CTG CTC **GCC** ATA GTG AGC AGG TGT CAC-3′; W296R, forward, 5′-C ATC ACT GTG AAC TTC **CGG** TAT AAG GGG GCT C-3′; reverse, 5′-G AGC CCC CTT ATA **CCG** GAA GTT CAC AGT GAT G-3′; L340R, forward, 5′-GTG GGG CCC TTG **AGG** AAC ACA ATG ATC AAG GGC-3′; reverse, 5′-GCC CTT GAT CAT TGT GTT **CCT** CAA GGG CCC CAC-3′. Bold codons indicate the site of mutation. The integrity of the mutations was confirmed by DNA sequencing.

Protein Production—Wild-type FIH, FIH mutants, and GST-HIF-1$\alpha_{786-826}$ were purified as described (11). Protein purity (>95%) was confirmed by SDS-PAGE analysis and electrospray ionization-mass spectrometry (MS) analyses.

Radiochemical Assays—Enzyme assays measured the release of [^{14}C]CO_2 from 1-[^{14}C]2OG (11). FIH variants (11.5 μM) were incubated with HIF-1$\alpha_{786-826}$ (57.5 μM) in the presence of 80 μM Fe(II), 160 μM 2OG, 4 mM ascorbate, and 1 mM dithiothreitol (DTT) in 50 mM Tris-HCl, pH 7.5 at 37 °C for 30 min. The final reaction volume was 100 μl. Under these conditions, ~50% of the HIF-1α substrate is hydroxylated by wild-type FIH. Reactions were quenched by the addition of 200 μl of methanol followed by a 30-min incubation on ice. Ascorbate analogs or alternative substrates (Sigma-Aldrich) were dissolved in Tris-HCl buffer (50 mM, pH 7.5) and tested in the 1-[^{14}C]2OG decarboxylation assay as reported above. For time course data, reactions were stopped at specific time points by quenching as described above. Assays monitoring oxygen depletion were carried out as described (19).

Hydroxylation Assays Using MALDI MS HIF—1$\alpha_{788-806}$ peptide substrate was obtained from Peptide Protein Research Ltd. (Fareham, UK). Reactions were carried out using the same conditions as for the radiochemical assays, except unlabeled 2OG was used and the final 2OG (500 μM) and Fe(II) (400 μM) concentrations were increased. Incubations in the presence of sodium carbonate, sodium formate, sodium acetate, sodium propionate, or sodium azide (1, 5, 10, 20, 50, 100, or 200 mM) were carried out. After incubation (30 min), trifluoroacetic acid (0.1% final concentration) was added, and the reaction mixture was diluted five times with double distilled water. For MS analyses, the quenched reaction mixtures (1 μl) were mixed with α-cyano-4-hydroxycinnamic acid (1 μl) and spotted onto a target plate. MALDI-time-of-flight spectra in the negative ion mode were then recorded for each sample.

Crystallography—The crystallization conditions for both FIH-D201A and FIH-D201G were similar to those described for wild-type FIH (17). The variants were crystallized (in a Belle Laboratories glove box under anaerobic conditions for FIH-D201A and aerobic conditions for FIH-D201G) by hanging drop vapor diffusion at 18 °C using 2-μl drops (1 μl of protein solution:1 μl of well solution) against a well solution of 0.1 M HEPES, pH 7.5, 1.6 M $(NH_4)_2SO_4$, and 6% polyethylene glycol 400. The FIH-D201A or FIH-D201G protein solution contained 14 or 25 mg/ml, respectively, in 50 mM Tris-HCl, pH 7.5, with 1 mM HIF-1$\alpha_{786-826}$ or 0.5 mM HIF-1$\alpha_{788-806}$ peptide, 1 mM $FeSO_4$, or $ZnCl_2$ and 2 mM 2OG (added under anaerobic conditions for FIH-D201A). Crystals were fully grown within 8 days. The crystals were removed from the glove box, transferred into a well solution containing 24% glycerol that was prepared in the glove box and immediately retrieved using a nylon loop, frozen by rapid plunging into liquid nitrogen, and stored under liquid nitrogen until data collection. The entire process of removing the crystals from the glove box through

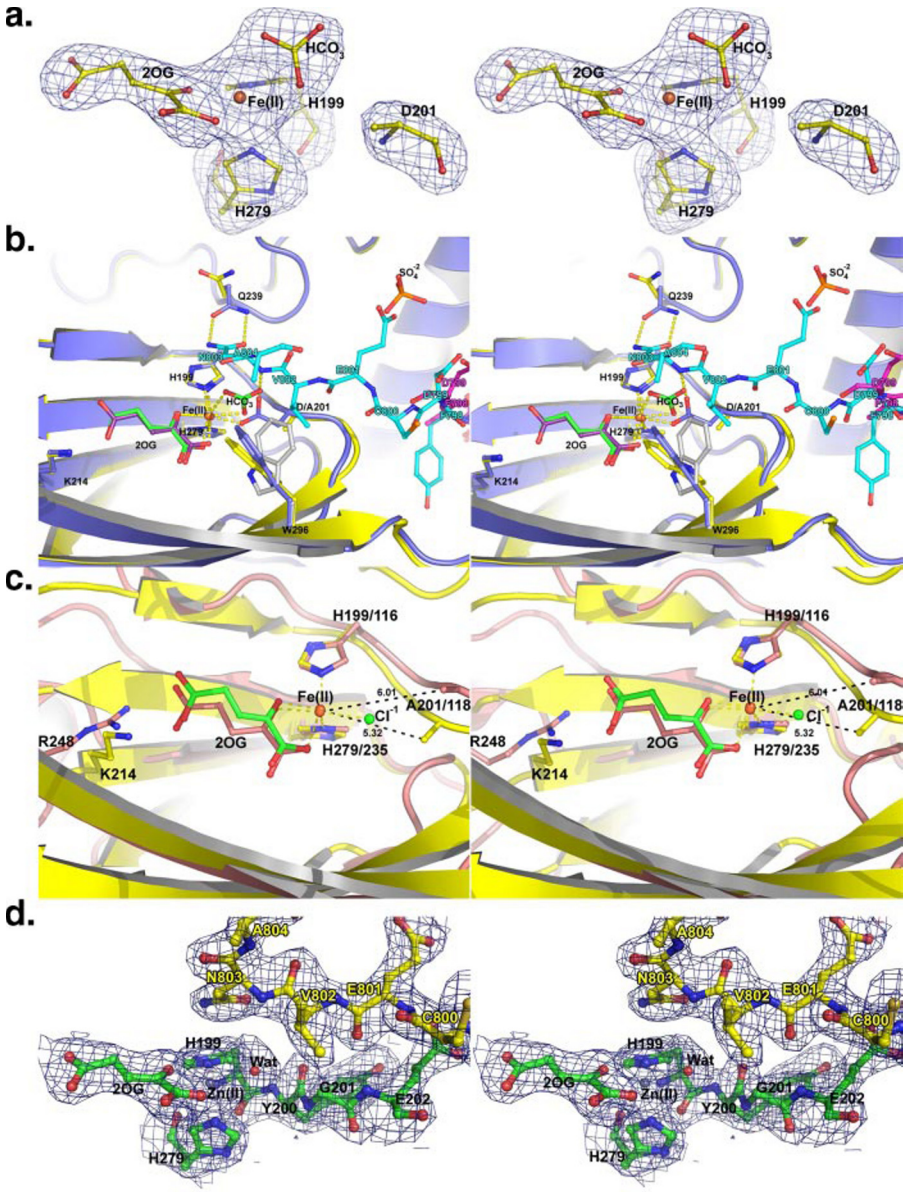

FIGURE 2. **Insights from crystal structures of FIH-D201A and FIH-D201G.** *a*, stereo view of the iron binding site of the FIH-D201A·Fe(II)·2OG·HIF-1$\alpha_{786-826}$ complex. Experimental electron density OMIT map ($F_o - F_c$) contoured to 5σ represented as *blue mesh* (electron density is carved out around the residues and ligands displayed for clarity). The unanticipated electron density adjacent to the iron was provisionally modeled as (bi)carbonate (see "Results" for discussion). *b*, comparison of the wild-type FIH·Fe(II)·2OG·HIF-1$\alpha_{786-826}$ complex (PDB ID 1H2L) with the FIH-D201A·Fe(II)·2OG·HIF-1$\alpha_{786-826}$ complex (wild-type FIH (*blue*) in complex with HIF substrate (*cyan*) and FIH-D201A (*yellow*) in complex with HIF substrate (*magenta*)). This figure emphasizes several important interactions between wild-type FIH and HIF-1α that are lost in the FIH-D201A complex: wild-type FIH Asp-201 and HIF-1α Asn-803 main chain nitrogen (*yellow dash*), wild-type FIH Gln-239 and HIF-1α Asn-803 side chain, and wild-type FIH Trp-296 and HIF-1α Val-802. Note the presence of the assigned sulfate ion (*orange* and *red*) in the FIH-D201A structure apparently replacing the carboxylate of the HIF-1α Glu-801 in the wild-type FIH·Fe(II)·2OG·HIF-1$\alpha_{786-826}$ complex, which is also observed in uncomplexed wild-type FIH structure (PDB 1H2N, not shown). *c*, stereo views from the crystal structures of 2OG-dependent halogenase, SyrB2 (*pink*) superimposed on the FIH-D201A variant (*yellow*). The FIH-D201A variant shares the same HXA . . . H motif as SyrB2 (PDB ID 2FCT); however, the FIH-D201A apparently does not provide enough space for a chloride ion to complete octahedral coordination to the Fe(II), which could explain why FIH-D201A does not have halogenase activity toward HIF-1α under our assay conditions. Distances between the FIH-D201A Ala-201 Cβ methyl group and Fe(II) in each of the structures are shown as *black dashed lines* to emphasize this point. *d*, stereo view ball-and-stick representation of the FIH-D201G·Zn(II)·2OG·HIF-1$\alpha_{786-826}$ complex metal binding site. Experimental electron density $2F_o - F_c$ contoured to 1.0σ represented as *blue mesh* (electron density is carved out around the residues and ligands displayed for clarity). FIH and 2OG are colored *green*, HIF-1$\alpha_{786-826}$ is colored *yellow*, Zn(II) is colored as a *gray sphere*, and the Zn(II) bound water is colored as a *red sphere*. *Wat*, water.

freezing took less than 5 min to minimize the diffusion of oxygen into the crystal-containing solution. Crystal-containing loops were mounted on a goniometer in a cryo-stream at 100 K. For FIH-D201A, 153 images of 1° oscillation, 15 s per image with a crystal to detector distance of 275 mm, were collected at the European Synchrotron Radiation Facility (ESRF) BM14 tuned to wavelength of 0.95372 Å using a MarMosiaic 225 CCD detector. For FIH-D201G, 360 images of 0.5° oscillation, 1 s per image, and a crystal to detector distance of 294 mm were used. Data were collected at Diamond I04 tuned to a wavelength of 0.9696 Å using an ADSC Quantum 315 CCD detector. Data were processed using HKL2000 (20) (supplemental Table S1).

To follow the refinement progress, a subset of 5% of the data was withheld from refinement throughout to obtain an R_{free} value. The coordinates from PDB entry 1H2N (17) were used as the starting model for one cycle of rigid body refinement followed by cycles of maximum likelihood-simulated annealing with bulk solvent correction using CNS version 1.1 (21) and model rebuilding using COOT version 0.26 (22) until convergence of R and R_{free}. Water molecules were placed based on $2F_o - F_c$ electron density peaks that were within hydrogen-bonding distance of protein donors or acceptors. The structure was analyzed for problem areas between refinement cycles using PROCHECK (23) and WHATIF (24). The structures have been deposited in the Research Collaboratory for Structural Bioinformatics (RCSB) PDB as PDB IDs 2ILM (FIH-D201A) and 3D8C (FIH-D201G).

RESULTS

Biochemical Characterization of FIH D201A—Consistent with the previous cell-based results (12), purified FIH-D201A did not catalyze hydroxylation of HIF peptide substrate (HIF-1$\alpha_{788-806}$) *in vitro*,

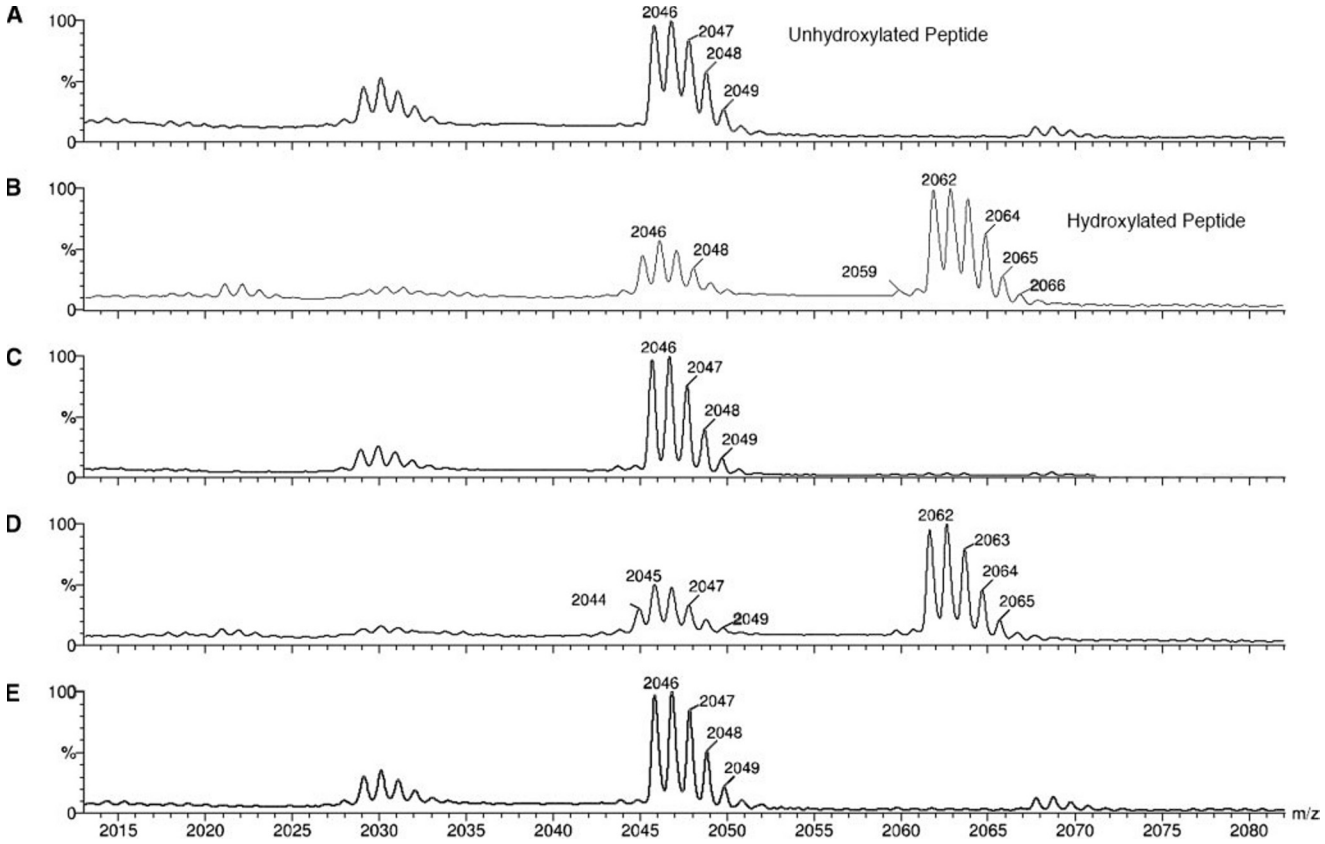

FIGURE 3. **Negative ion MALDI-time-of-flight analysis of 19-mer HIF-1α C-terminal transactivation domain peptide (HIF-1$\alpha_{788-806}$) incubated with standard 2OG and Fe(II) conditions.** *A*, HIF-1$\alpha_{788-806}$ peptide substrate only. *B*, HIF-1$\alpha_{788-806}$ peptide incubated with wild-type FIH. *C*, HIF-1$\alpha_{788-806}$ peptide incubated with FIH-D201A. *D*, HIF-1$\alpha_{788-806}$ peptide incubated with FIH-D201G. *E*, HIF-1$\alpha_{788-806}$ peptide incubated with the FIH-D201G/W296R double variant. Unhydroxylated HIF-1$\alpha_{788-806}$ peptide shows peaks at 2046–2050 Da with hydroxylated HIF-1$\alpha_{788-806}$ peptide showing peaks at 2062–2065 Da. The peak group at 2030 Da is due to an impurity in the substrate.

as demonstrated by MS analyses (Fig. 3). However, using an assay in which the amount of $[^{14}C]CO_2$ produced from 1-[^{14}C]2OG is used to measure activity, significant stimulation of 2OG turnover by the FIH-D201A variant was observed under standard assay conditions in the presence of ascorbate (supplemental Fig. S1). For FIH-D201A, the extent of 2OG decarboxylation was greater than for wild-type FIH, with all of the 2OG in the reaction mixture being consumed in the FIH-D201A assay. Under the same conditions, wild-type FIH catalyzed hydroxylation of ~50% of the HIF-1α substrate and decarboxylated only ~15% of the 2OG present (Fig. 4). Attempts to restore the wild-type hydroxylase activity with the FIH-D201A mutant by the use of small molecules (formate, acetate, propionate, carbonate, and azide) in assays with HIF-1$\alpha_{788-806}$ were unsuccessful (supplemental Fig. S3).

Ascorbate and HIF-1α Dependence—Ascorbate has relatively little effect on wild-type FIH activity. Unexpectedly, when using HIF-1$\alpha_{786-826}$ as a substrate for FIH-D201A, it was found that the addition of L-ascorbate was a requirement for enhanced 2OG turnover, stimulating activity ~10-fold. Furthermore, the 2OG turnover activity of FIH-D201A was reduced (~10-fold) in the absence of HIF-1$\alpha_{786-826}$ substrate, implying that both ascorbate and HIF-1$\alpha_{786-826}$ substrate are required for efficient 2OG decarboxylation (Fig. 4) despite the absence of HIF-1$\alpha_{788-806}$ hydroxylation. For both wild-type FIH and FIH-D201A, activity was reduced in the absence of added Fe(II).

Substrate Mutations—The relative importance of HIF-1α Asn-803, the normally hydroxylated residue, to FIH activity has been reported (25). FIH does not stimulate 2OG turnover (<0.1% of wild-type GST-HIF-1$\alpha_{786-826}$) in the presence of the GST-HIF-1$\alpha_{786-826}$-N803A, -N803E, and -N803Q variants. The GST-HIF-1$\alpha_{786-826}$-N803D variant resulted in only ~7% 2OG turnover when compared with that of WT-GST-HIF-1$\alpha_{786-826}$ with FIH (11). The effects of the same GST-HIF-1$\alpha_{786-826}$ variants on FIH-D201A activity were investigated; they all stimulated 2OG turnover to approximately the same level: N803A (18% of wild-type GST-HIF-1$\alpha_{786-826}$ activity observed), N803D (20%), N803E (17%), and N803Q (16%).

Dimerization Dependence—The FIH-L340R substitution has been shown to convert the FIH homodimer into a predominantly monomeric form that shows ~20% of the wild-type FIH 2OG turnover activity but is inactive with respect to HIF hydroxylation (26). To investigate whether the homodimeric form of FIH-D201A was required for the uncoupled 2OG turnover, the double mutant FIH-D201A/L340R was prepared and analyzed. FIH-D201A/L340R did not stimulate 2OG turnover in the presence of L-ascorbate and/or HIF-1α, indicating that, as for wild-type FIH, the homodimeric form of FIH-D201A is required for catalysis (Fig. 4).

Ascorbate Analogs—To investigate the specificity of FIH-D201A for ascorbate, ascorbate analogs were tested using the [^{14}C]2OG decarboxylation assay. D-Isoascorbate gave ~75%

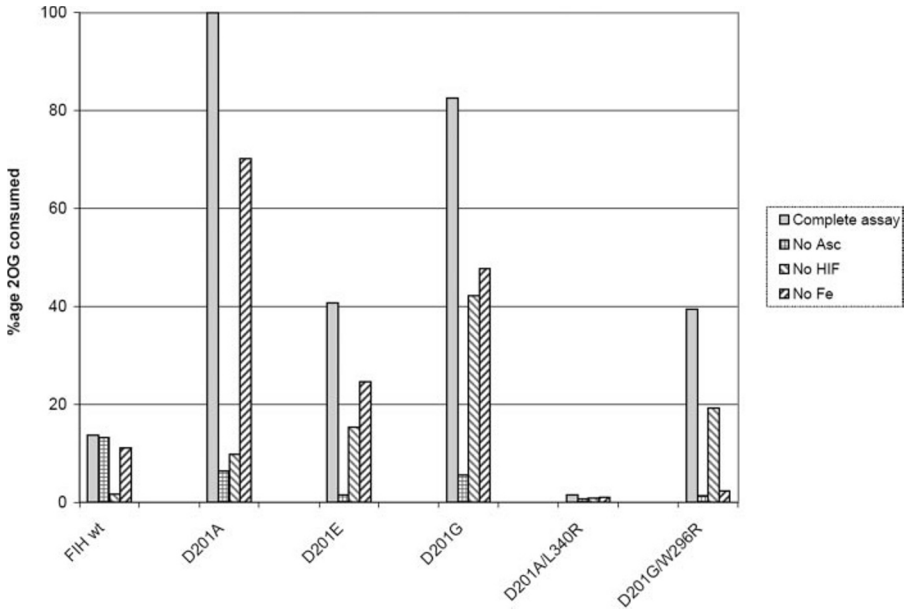

FIGURE 4. **1-[^{14}C]2OG turnover assay data for FIH-D201A, FIH-D201E, FIH-D201G, FIH-D201A/L340R, and FIH-D201G/W296R mutants when compared with the wild-type FIH.** The *bars* (±5% error) indicate the amount (decompositions per minute) of radiolabeled [^{14}C]CO_2 collected after incubation. *%age*, percentage. *No Asc*, no ascorbate.

(±5% error) of the activity of L-ascorbate for FIH-D201A. L-Galactonic acid-γ-lactone, L-gulonic-γ-lactone, and L-mannonic acid-γ-lactone all stimulated 2OG turnover by only ~5% of the level observed for L-ascorbate with FIH-D201A; these results indicate the importance of the dienol moiety of ascorbate. Interestingly, isopropylidene-L-ascorbic acid stimulated FIH-D201A activity to the same level as L-ascorbate, but (+)-5,6-O-cyclohexylidene-L-ascorbic acid to only ~8%, suggesting a steric constraint on ascorbate-dependent oxidation.

Further evidence for the selectivity of reducing agent came from the observation that DTT effectively substituted for L-ascorbate (~95% activity), but dithionite, β-mercaptoethanol, and tris-(2-carboxyethyl)phosphine hydrochloride all stimulated activity to less than 10% (~3, 9, and <1%, respectively) of that observed for L-ascorbate and DTT. Since phenol and its derivatives have been used both as alternative substrates and as competitive inhibitors of the copper-dependent ascorbate oxidase (27), phenol and selected phenolic derivatives (4-chlorophenol, 4-nirophenol, 4-cyanophenol, 4-tertbutylphenol, 4-methylphenol, 1,2-dihydroxybenzene, 4-nitrocatechol) were tested both as ascorbate substitutes and as inhibitors of FIH-D201A. None of the phenolic compounds could replace ascorbate as stimulators of FIH-D201A activity or were found to be potent inhibitors.

FIH-D201E—Given that the structurally characterized 2OG-dependent dioxygenases (JMJD2A and clavaminic acid synthase) have a glutamic acid residue functioning as the carboxylate iron binding ligand (28, 29), the FIH-D201E variant was investigated. The FIH-D201E had low 2OG turnover activity in the absence of ascorbate, and MS analyses showed that this mutant did not support HIF-1$\alpha_{788-806}$ hydroxylation. However, FIH-D201E did catalyze the turnover of 2OG (to a lesser extent than FIH-D201A), which was stimulated by the addition of L-ascorbate and GST-HIF-1$\alpha_{786-826}$ (Fig. 4).

FIH-D201G and FIH-D201G/W296R—To further probe the role of the carboxylate residue of the facial triad in FIH, a glycyl residue was substituted for Asp-201. The FIH-D201G mutant behaved similarly to FIH-D201A in that 2OG decarboxylation was highly dependent on the presence of L-ascorbate. 2OG turnover by FIH-D201G was less dependent on GST-HIF-1$\alpha_{786-826}$ when compared with FIH-D201A (Fig. 4). An unanticipated result was that, in contrast to FIH-D201A and FIH-D201E, FIH-D201G supported HIF-1$\alpha_{788-806}$ hydroxylation (as shown by MS assays) at levels comparable with wild-type FIH (Fig. 3). A FIH-D201G/W296R double variant was also generated because an arginine occupies the equivalent position as the FIH Trp-296 at the active site of the SyrB2 2OG-dependent halogenase (8). Catalysis of HIF-1$\alpha_{788-806}$ hydroxylation by the double variant was not detected by MS analyses (Fig. 3), possibly because the substitution of the hydrophobic tryptophan with a polar/charged arginine probably disrupts the interaction with Val-802 of HIF1α (17). For the double variant, 2OG decarboxylation was observed, but to a lesser extent than that observed with the D201A variant. 2OG turnover was highly dependent on the presence of L-ascorbate but was less dependent on the presence of HIF-1$\alpha_{786-826}$ when compared with D201A (Fig. 4). As for FIH-D201A and FIH-D201G, activity of FIH-D201G/W296R was stimulated by the addition of Fe(II).

Crystal Structures of FIH-D201A and FIH-D201G in Complex with HIF-1α Substrate—To examine the mode of metal coordination in FIH-D201A and FIH-D201G, crystallographic analyses were performed. Attempts to crystallize the D201E mutant failed, so modeling of this variant was carried out (supplemental Fig. S2).

FIH-D201A crystals were grown in the presence of Fe(II), 2OG, and HIF-1$\alpha_{786-826}$ under anaerobic conditions by the hanging drop vapor diffusion method. Synchrotron data were collected to 2.3 Å resolution and refined to a final R_{factor} of 21.0% and R_{free} of 26.7%. FIH-D201G crystals were grown in the presence of Zn(II), 2OG, and HIF-1$\alpha_{788-806}$ by the hanging drop vapor diffusion method. Synchrotron data were collected to 2.1 Å resolution and refined to a final R_{factor} of 21.8% and R_{free} of 25.6%.

Overall, the structures of the FIH mutants in complex with HIF-1α are very similar to that of the wild-type FIH·Fe(II)·2OG·HIF-1$\alpha_{786-826}$ complex (PBD ID 1H2L (17)) (Fig. 2, *a* and *b*). However, there are significant differences with respect to the binding of HIF-1α substrate. In contrast to the wild-type structure, which shows HIF-1α residues binding at two sites, residues 795–806 (site 1 as defined in Elkins *et al.* (17)) and 813–822 (site 2), only HIF-1α residues 794–799

from site 1 are observed in the FIH-D201A·Fe(II)·2OG·HIF-1$\alpha_{786-826}$ complex, and HIF-1α residues 794–806 from site 1 are observed in the FIH-D201G·Zn(II)·2OG·HIF-1$\alpha_{788-806}$ complex (Fig. 2*d*).

In both FIH-D201 variant structures, the active site metal is coordinated by only two enzyme-derived residues (His-199 and His-279) that adopt near identical conformations to those in the wild-type FIH structures. The main-chain atoms of residue 201 overlay with those of the wild-type structure (Fig. 2, *a* and *b*). In both variant structures, the 2OG is coordinated to the Fe(II) in a similar manner to wild-type FIH with its 1-carboxylate group binding *trans* to His-199. However, the electron density map of the FIH-D201A·Fe(II)·2OG·HIF-1$\alpha_{786-826}$ structure indicated an additional planar metal ligand, possibly comprised of four atoms bound to Fe(II) in a bidentate manner that apparently distorts the typical octahedral metal coordination geometry. This apparent ligand, provisionally assigned as a carbonate or bicarbonate ion, is possibly derived from CO_2, generated by 2OG (30), but other possibilities including acetate or a HIF-1α-derived species cannot be ruled out. One of the two assigned Fe(II)-ligated oxygen atoms of the (bi)carbonate approximately bisects the position of the two carboxylate oxygens of Asp-201 in wild-type FIH and has an apparently longer coordination bond length (2.5 Å) than the other Fe(II)-coordinating atoms ($\leq$ 2.4 Å).

In the FIH-D201A·Fe(II)·2OG·HIF-1$\alpha_{786-826}$ structure, there was reasonable occupancy for residues 794–799 of HIF-1α in site 1, and comparison with the wild-type FIH·Fe(II)·2OG·HIF-1$\alpha_{786-826}$ complex reveals that this region of the HIF-1α peptide adopts a similar conformation in both structures (Fig. 2*d*). This region of HIF-1α binds close to the FIH dimer interface formed by the two C-terminal helices (26). However, HIF-1α residues (800–806 in PDB ID 1H2L) near the iron binding site in the FIH-D201A·Fe(II)·2OG·HIF-1$\alpha_{786-826}$ structure are probably disordered, as observed by broken residual difference density that did not refine well, even when defined with a low occupancy.

To investigate why the FIH-D210G but not the FIH-D201A can catalyze hydroxylation, a crystal structure was also obtained for the FIH-D210G·Zn(II)·2OG·HIF-1$\alpha_{788-806}$ complex (Fig. 2*d*). In contrast to the FIH-D201A·Fe(II)·2OG·HIF-1$\alpha_{786-826}$ structure, the FIH-D201G structure reveals the HIF-1$\alpha_{788-806}$ substrate positioned similarly to that of the WT-FIH·Fe(II)·2OG·HIF-1$\alpha_{786-826}$ complex in site 1 (Fig. 2*d*), such that Asn-803 is adjacent to the active site metal (Zn(II) substituting for Fe(II)).

Overall, the crystallographic results imply that only two enzyme-derived iron-coordinating ligands are required for 2OG turnover and hydroxylation. Although it is possible that the differences may result from crystallographic artifacts, the different binding modes observed for HIF-1$\alpha_{786-826}$ in the FIH-D201A and the WT FIH/FIH-D201G correlate with the lack of hydroxylation activity observed for FIH-D201A. The non-productive binding of HIF-1$\alpha_{786-826}$ in FIH-D201A crystals may be related to the apparent metal ligand observed for this variant because it is in position to interfere with substrate binding.

DISCUSSION

Although we cannot entirely exclude the possibility of a rearrangement in solution to provide a third protein based Fe(II) ligand, the biochemical and crystallographic results presented here provide evidence that only two His-residues are required for FIH-D201A/G to bind iron and 2OG to catalyze the oxidative decarboxylation of 2OG to succinate and carbon dioxide.

In contrast to the wild-type and FIH-D201G HIF substrate complex structures, density for HIF-1α Asn-803 and the surrounding residues (800–806) was not observed adjacent to the iron center in the FIH-D201A substrate complex. Although we cannot be certain that this reflects the situation in solution, the presence of a methyl side chain at FIH residue-201 must hinder productive binding. The difference in the hydroxylation activity between the FIH-D201A and FIH-D201G cannot solely result from steric effects because in wild-type FIH residue-201 is an aspartate. It is possible that the presence of a glycine, rather than an alanine residue, enables complexation of a water molecule to the iron that can hydrogen-bond to HIF-1α Asn-803 in a analogous manner to that observed for Asp-201 in the wild-type FIH-HIF structural complex.

The FIH-D201A mutant resembles the SyrB2 2OG-dependent chlorinating enzyme, of which the iron is also coordinated by two His-residues with an Ala residue in a similar position as residue 201 in FIH (7). During catalysis by SyrB2, a halide ion replaces the iron coordination site occupied by the side-chain carboxylate of Asp-201 in FIH (Fig. 2*c*) (8). Attempted chlorination of the HIF-1α substrate by FIH-D201A in assays supplemented with sodium chloride was unsuccessful. Structural comparison of FIH-D201A with SyrB2 suggests that this may in part be due to a lack of space for the chloride ion to coordinate Fe(II) (Fig. 2*c*). Although our attempted halogenation experiments were negative, the knowledge that FIH-D201G only requires two enzyme-derived iron ligands opens the way for studies aimed at further modifying FIH to enable the halogenation of unactivated C–H bonds in proteins.

In light of the discovery of the 2OG chlorinating enzymes (7, 8) and the results described here for the FIH-D201A mutant, consideration should be given to the possibility of an Fe(II)-coordinating "two-histidine dyad" in searches for 2OG oxygenases in bioinformatic-based approaches. Other variants of the facial triad may also exist; modeling of the JmjC domain of the fission yeast protein Epe1, thought to be a 2OG-dependent hydroxylase (31), using an alignment with FIH, indicates that the second His residue of the facial triad is replaced by Tyr (32). Thus the predicted iron-coordinating residues in Epe1 are His, Glu, and Tyr (H*X*E . . . Y). Sequence analyses also imply that the H*X*(D/E) . . . H facial triad may not be conserved in other 2OG-dependent dioxygenases, including the epidermal growth factor aspartyl/asparaginyl hydroxylase (33).

The FIH-D201A/E variants do not catalyze HIF-1α asparaginyl hydroxylation, but do catalyze decarboxylation of 2OG, and at a higher rate than that observed for the wild-type FIH. However, unlike the hydroxylation reaction catalyzed by wild-type FIH with HIF-1α C-terminal transactivation domain, the oxidation of 2OG by both FIH-D201G/A mutants was very dependent on the presence of a reducing

agent, such as ascorbate or DTT. In the case of FIH-D201G, 2OG turnover was coupled, at least partially, to substrate hydroxylation. However, in contrast to wild-type FIH, for FIH-D201G, both 2OG decarboxylation in the absence of substrate and HIF substrate hydroxylation were ascorbate-dependent. This dependence resembles that of some other 2OG oxygenases (see *e.g.* Refs. 34 and 35), including collagen prolyl hydroxylase, the activity of which is well known to be stimulated by ascorbate.

It is reasonable to propose that the first part of the catalytic cycles for both the wild-type FIH and the FIH-D201X mutants is common, *i.e.* 2OG is oxidized to produce succinate, carbon dioxide, and an Fe(VI)=O intermediate (36, 37). Because HIF-1α is not hydroxylated by the FIH-D201A/E mutants, regeneration of Fe(II) from the higher oxidation state intermediates is required to complete their catalytic cycle. The requirement for a reducing agent may in part rationalize the increased dependence of these FIH variants on ascorbate when compared with WT FIH. It is also possible that, in addition to completing some catalytic cycles, ascorbate affects the reactivity of intermediate complexes.

Substitutions of iron binding residues or other active site residues of 2OG-dependent dioxygenases have been reported (38, 39) to (partially) decouple 2OG and prime substrate oxidation. However, the increased 2OG turnover by the D201A/E/G variants of FIH is unusual. In FIH, Asp-201 is proposed to play a role both in binding iron and in accepting a hydrogen bond from HIF Asn-803, the substrate residue that is hydroxylated. A third possible role for Asp-201 is in hindering binding of oxygen prior to that of HIF substrate. The non-iron-ligating side-chain carboxylate oxygen may stabilize binding of a water molecule to the five coordinate FIH·Fe·2OG complex, giving a relatively stable six-coordinate complex (as proposed for other 2OG oxygenases (4)). On substrate binding, a five-coordinate complex is formed that can react with oxygen and in which the non-ligating oxygen of Asp-201 hydrogen bonds with Asn-803 of HIF. This mechanism could prevent FIH-mediated non-productive 2OG turnover when HIF substrate is not available. Substitutions of FIH Asp-201 may result in a weakened interaction between the water molecule and Fe(II) in the FIH-D201A/E·Fe(II)·2OG complexes, making reaction with oxygen easier and causing the high levels of 2OG turnover observed for these variants in the absence of HIF.

Significantly, despite the fact the methyl side chain of Ala-201 can neither covalently bind the iron nor hydrogen-bond to the substrate, the 2OG turnover activity of FIH-D201A was stimulated by the presence of HIF-1$\alpha_{786-826}$. Since the HIF-1$\alpha_{786-826}$ was not itself hydroxylated by FIH-D201A, the results imply that the oxidation of 2OG is catalyzed by a hybrid complex comprised of FIH-D201A and HIF-1$\alpha_{786-826}$. It is possible that the selectivity of this hybrid complex could be engineered by synthetic modifications to the HIF-1$\alpha_{786-826}$ component. The HIF-1$\alpha_{786-826}$-stimulating effect was seen to a much lesser extent with the D201E FIH mutant, possibly because this mutant can still bind iron via a triad of FIH-derived residues; the larger glutamyl side chain may also limit space available for substrate (peptide or ascorbate) binding.

The increased 2OG turnover activity observed for FIH-D201A in the presence of HIF-1$\alpha_{786-826}$ substrate may in part be because the HIF-1α substrate modifies the FIH active site to strengthen Fe(II) binding. However, the structural studies suggest that such an effect may be more complicated than strengthening of iron binding via a direct complexation. Although the detailed mechanism by which HIF-1α peptides stimulate 2OG turnover by FIH-D201A is complicated, the available evidence implies that it may also include binding interactions away from the immediate vicinity of the Fe(II) including those at, or close to, the dimer interface.

REFERENCES

1. Clifton, I. J., McDonough, M. A., Ehrismann, D., Kershaw, N. J., Granatino, N., and Schofield, C. J. (2006) *J. Inorg. Biochem.* **100,** 644–669
2. Costas, M., Mehn, M. P., Jensen, M. P., and Que, L., Jr. (2004) *Chem. Rev.* **104,** 939–986
3. Hausinger, R. P. (2004) *CRC Crit. Rev. Biochem. Mol. Biol.* **39,** 21–68
4. Neidig, M. L., Brown, C. D., Light, K. M., Fujimori, D. G., Nolan, E. M., Price, J. C., Barr, E. W., Bollinger, J. M., Jr., Krebs, C., Walsh, C. T., and Solomon, E. I. (2007) *J. Am. Chem. Soc.* **129,** 14224–14231
5. Lange, S. J., and Que, L., Jr. (1998) *Curr. Opin. Chem. Biol.* **2,** 159–172
6. Galonic, D. P., Barr, E. W., Walsh, C. T., Bollinger, J. M., Jr., and Krebs, C. (2007) *Nat. Chem. Biol.* **3,** 113–116
7. Vaillancourt, F. H., Yin, J., and Walsh, C. T. (2005) *Proc. Natl. Acad. Sci. U. S. A.* **102,** 10111–10116
8. Blasiak, L. C., Vaillancourt, F. H., Walsh, C. T., and Drennan, C. L. (2006) *Nature* **440,** 368–371
9. Bruick, R. K., and McKnight, S. L. (2001) *Science* **294,** 1337–1340
10. Epstein, A. C., Gleadle, J. M., McNeill, L. A., Hewitson, K. S., O'Rourke, J., Mole, D. R., Mukherji, M., Metzen, E., Wilson, M. I., Dhanda, A., Tian, Y. M., Masson, N., Hamilton, D. L., Jaakkola, P., Barstead, R., Hodgkin, J., Maxwell, P. H., Pugh, C. W., Schofield, C. J., and Ratcliffe, P. J. (2001) *Cell* **107,** 43–54
11. Hewitson, K. S., McNeill, L. A., Riordan, M. V., Tian, Y. M., Bullock, A. N., Welford, R. W., Elkins, J. M., Oldham, N. J., Bhattacharya, S., Gleadle, J. M., Ratcliffe, P. J., Pugh, C. W., and Schofield, C. J. (2002) *J. Biol. Chem.* **277,** 26351–26355
12. Lando, D., Peet, D. J., Gorman, J. J., Whelan, D. A., Whitelaw, M. L., and Bruick, R. K. (2002) *Genes Dev.* **16,** 1466–1471
13. Lando, D., Peet, D. J., Whelan, D. A., Gorman, J. J., and Whitelaw, M. L. (2002) *Science* **295,** 858–861
14. Kaelin, W. G., Jr. (2004) *Clin. Cancer Res.* **10,** 6290S–6295S
15. Hewitson, K. S., Granatino, N., Welford, R. W., McDonough, M. A., and Schofield, C. J. (2005) *Philos. Transact. A Math. Phys. Eng. Sci.* **363,** 807–828
16. Dann, C. E., III, Bruick, R. K., and Deisenhofer, J. (2002) *Proc. Natl. Acad. Sci. U. S. A.* **99,** 15351–15356
17. Elkins, J. M., Hewitson, K. S., McNeill, L. A., Seibel, J. F., Schlemminger, I., Pugh, C. W., Ratcliffe, P. J., and Schofield, C. J. (2003) *J. Biol. Chem.* **278,** 1802–1806
18. Lee, C., Kim, S. J., Jeong, D. G., Lee, S. M., and Ryu, S. E. (2003) *J. Biol. Chem.* **278,** 7558–7563
19. Ehrismann, D., Flashman, E., Genn, D. N., Mathioudakis, N., Hewitson, K. S., Ratcliffe, P. J., and Schofield, C. J. (2007) *Biochem. J.* **401,** 227–234
20. Otwinowski, Z., and Minor, W. (1997) *Methods Enzymol.* **276,** 307–326
21. Brunger, A. T., Adams, P. D., Clore, G. M., DeLano, W. L., Gros, P., Grosse-Kunstleve, R. W., Jiang, J. S., Kuszewski, J., Nilges, M., Pannu, N. S., Read, R. J., Rice, L. M., Simonson, T., and Warren, G. L. (1998) *Acta Crystallogr. Sect. D Biol. Crystallogr.* **54,** 905–921
22. Emsley, P., and Cowtan, K. (2004) *Acta Crystallogr. Sect. D Biol. Crystallogr.* **60,** 2126–2132
23. Laskowski, R. A., MacArthur, M. W., Moss, D. S., and Thornton, J. M. (1993) *J. Appl. Crystallogr.* **26,** 283–291
24. Vriend, G. (1990) *J. Mol. Graph.* **8,** 52–56
25. Cockman, M. E., Lancaster, D. E., Stolze, I. P., Hewitson, K. S., McDonough, M. A., Coleman, M. L., Coles, C. H., Yu, X., Hay, R. T., Ley,

S. C., Pugh, C. W., Oldham, N. J., Masson, N., Schofield, C. J., and Ratcliffe, P. J. (2006) *Proc. Natl. Acad. Sci. U. S. A.* **103,** 14767–14772
26. Lancaster, D. E., McNeill, L. A., McDonough, M. A., Aplin, R. T., Hewitson, K. S., Pugh, C. W., Ratcliffe, P. J., and Schofield, C. J. (2004) *Biochem. J.* **383,** 429–437
27. Gaspard, S., Monzani, E., Casella, L., Gullotti, M., Maritano, S., and Marchesini, A. (1997) *Biochemistry* **36,** 4852–4859
28. Zhang, Z., Ren, J., Stammers, D. K., Baldwin, J. E., Harlos, K., and Schofield, C. J. (2000) *Nat. Struct. Biol.* **7,** 127–133
29. Chen, Z., Zang, J., Whetstine, J., Hong, X., Davrazou, F., Kutateladze, T. G., Simpson, M., Mao, Q., Pan, C. H., Dai, S., Hagman, J., Hansen, K., Shi, Y., and Zhang, G. (2006) *Cell* **125,** 691–702
30. Neidig, M. L., and Solomon, E. I. (2005) *Chem. Commun.* 5843–5863
31. Trewick, S. C., Minc, E., Antonelli, R., Urano, T., and Allshire, R. C. (2007) *EMBO J.* **26,** 4670–4682
32. Trewick, S. C., McLaughlin, P. J., and Allshire, R. C. (2005) *EMBO Rep.* **6,** 315–320
33. Lancaster, D. E., McDonough, M. A., and Schofield, C. J. (2004) *Biochem. Soc. Trans.* **32,** 943–945
34. Knowles, H. J., Raval, R. R., Harris, A. L., and Ratcliffe, P. J. (2003) *Cancer Res.* **63,** 1764–1768
35. Myllyla, R., Majamaa, K., Gunzler, V., Hanauske-Abel, H. M., and Kivirikko, K. I. (1984) *J. Biol. Chem.* **259,** 5403–5405
36. Price, J. C., Barr, E. W., Tirupati, B., Bollinger, J. M., Jr., and Krebs, C. (2003) *Biochemistry* **42,** 7497–7508
37. Proshlyakov, D. A., Henshaw, T. F., Monterosso, G. R., Ryle, M. J., and Hausinger, R. P. (2004) *J. Am. Chem. Soc.* **126,** 1022–1023
38. Myllyharju, J., and Kivirikko, K. I. (1997) *EMBO J.* **16,** 1173–1180
39. Sim, J., and Sim, T. S. (2000) *Biosci. Biotechnol. Biochem.* **64,** 828–832